Measurements of Sonoluminescence Temporal Pulse Shape

Michael J. Moran and Daren Sweider
Lawrence Livermore National Laboratory, Livermore, California 94550
(Received 30 December 1997)

Experiments using time-correlated photon counting and optical bandpass filters measure new features in the time and spectral dependences of single-bubble sonoluminescence (SBSL). The SBSL full width at half maximum (FWHM) varies with wavelength at 3 °C, but not at 24 °C. The pulse shapes are dominated by nearly Gaussian peaks with FWHM in the 150- to 300-ps range. At 3 °C, increases of pulse width with acoustic drive pressure are independent of wavelength. The pulses have extended tails that decay exponentially, with effective lifetimes of about 150 ps. [S0031-9007(98)06241-3]

PACS numbers: 78.60.Mq, 43.25.+y, 43.35.+d

Single-bubble sonoluminence (SBSL) emits brief flashes of light from a submerged gaseous bubble, which collapses repeatedly under the influence of a converging acoustic pressure wave. With the basic technique developed by Gaitan [1], a micron-sized air bubble in a water-filled piezoelectric-driven acoustic resonator produces a repeating train of SBSL. The flashes, with subnanosecond durations, submicron source sizes, "bluish" spectra that increase aggressively into the near uv, and integrated fluxes of about 10^5 to 10^6 photons, have been studied extensively [2]. Much has been learned about SBSL, but explanations of the mechanisms responsible for the light emission remain incomplete. The study of SBSL would be advanced further still by detailed measurements of the temporal shape of the light pulses. Such data could help to establish definite ties to theoretical predictions and ultimately help to explain the light-emission mechanisms.

An elegant paper by B. Gompf *et al.* [3] described the first use of time-correlated single-photon counting (TCPC) to resolve SBSL pulse widths of 60 to 250 ps for an air bubble in water at room temperature. Their TCPC apparatus, with an impulse response width of 49 ps, recorded autocorrelations of the SBSL pulse shape. The SBSL autocorrelation had a nearly Gaussian time profile whose full width at half maximum (FWHM) increased both with applied acoustic power and with dissolved gas concentration, but was unchanged when measured through optical bandpass filters centered at 320 and 620 nm. Using a similar TCPC method and a wide variety of experimental conditions, recent work by Hiller *et al.* [4] finds FWHM from 40 to 380 ps; finding also that the FWHM are independent of wavelength from 200 to 800 nm.

The present paper reports further measurements with a TCPC method that measures the actual SBSL pulse shape, rather than an autocorrelation. The present method records data quickly, resulting in excellent statistics ($\approx$7% uncertainty at 1% of the pulse peak height) and minimizing the problems with stability that have been endemic to SBSL experiments. The true SBSL pulse shapes can be extracted from the raw data by deconvolution of the TCPC instrument response function (IRF).

TCPC uses the timing of optical signals to sample the time dependence of fast optical pulses [5]. TCPC requires a "start" pulse timing marker and a detector to generate a "stop" timing signal that corresponds to a single photon from the pulse. The correlation between these 2 times over many pulses is recorded as a temporal distribution. If the start signal comes also from a second identical single-photon detector [3,4], the temporal distribution is an autocorrelation of the pulse shape. Here, data acquisition can be very slow because both single-photon detectors must contribute to each data point. When the start is a "trigger" that corresponds with the emission time of each optical pulse (as in the present experiment), the recorded distribution represents an average of the SBSL pulse shape. Here, with only one single-photon detector, data acquisition can be much faster.

Figure 1 is a schematic diagram of the present TCPC system. The Hamamatsu 3809U microchannel photomultipliers (MCP) have transit-time spreads of less than 40 ps and impulse response widths of about 250 nsec. The "multiphoton" MCP generates a start timing signal with many (>100) photoelectrons from each SBSL flash. The "single-photon" MCP generates stop signals that sample the SBSL pulse shape. Ortec 9306 1-GHz preamplifiers provide gain for the MCP signals and produce highly consistent and nearly Gaussian 400-ps

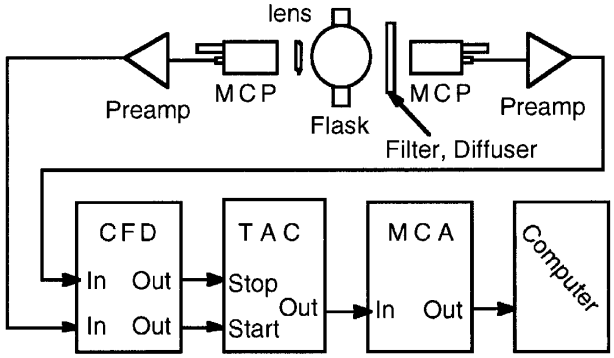

FIG. 1. Electronics for TCPC sampling of SBSL time dependence.

output pulses. Tennelec 454 constant fraction discriminators with carefully tuned internal delay jumpers convert the preamplifier pulses to timing signals. A standard time-to-amplitude converter (Ortec 457) and analog-to-digital converter (Oxford Instruments) convert the start-stop delays to corresponding pulse heights that are stored on a computer.

Measurements of subpicosecond (fs) 400-nm laser pulses characterize the IRF of the TCPC system. The IRF shown in Fig. 2 (solid line) is a smoothed fit to data (points) recorded with a dispersion of 6.25 ps/channel (ps/ch); the inset is a semilog plot of the raw data and fit. The "shoulder" at about 350 ps, with an amplitude of about 1.5% of the peak, is an inherent MCP characteristic. The shoulder is important because it can cause noticeable distortion of measured pulse shapes.

The present TCPC method requires a reliable start trigger from the multiphoton detector. The start trigger jitter (dashed curve in Fig. 2) is the same with SBSL and the fs laser. The jitter is instrument limited, is not broadened by SBSL pulses, varies from 47 to 53 ps for the data shown below, and corresponds to an uncertainty of about 36 ps for a single MCP. This precision, which matches the single-photon timing, is achievable only when the SBSL has a bright, stable bubble. This makes the measurements at 24 °C more difficult than at 3 °C, where the bubble is about one decade brighter [2]. The start timing jitter is monitored before and after experimental runs, using SBSL flashes as the light source.

The SBSL apparatus consists of a 6.5-cm-diameter quartz flask driven by two opposed piezoelectric transducers at the "breathing mode" frequency of 29 kHz. Distilled and deionized water, degassed in air to a pressure of 125 torr at room temperature, fills the flask to the bottom of the 3-mm bore of the neck, and is maintained either at 24 or 3 °C during SBSL runs. The flask is shrouded by black cloth, eliminating reflections from external components. A small acoustic probe placed just below the surface of the water provides a signal that is useful for monitoring SBSL conditions during an experiment. This signal is used during spectral or acoustic-pressure scans to maintain constant acoustic drive pressure.

Regarding experimental consistency, SBSL is highly sensitive to minute changes in experimental parameters and is notorious for difficulties with recording reproducible results [6]. The present apparatus does not allow *in situ* measurement of dissolved gas concentration, and the concentration may vary significantly over periods of about 30 min. Because of variation in resonance characteristics, even the applied acoustic power cannot always be reproduced exactly. In spite of these difficulties, consistent data can be recorded. Typically, for a series of measurements in a given "run" (e.g., using Melles-Griot 40-nm bandpass optical interference filters at 750, 550, 400, and 250 nm), each measurement is repeated at different times in the series. If the data are not consistent (i.e., appropriate FWHM agree within ± 10 ps), then the series is repeated. Unless otherwise stated, the data are recorded with a dispersion of 25 ps/ch at a single-photon counting rate of about 1000 counts per second, reaching about 20 000 counts at the signal peak after about five minutes.

Figure 3 shows the shape of the SBSL pulse recorded at 24 °C without optical filtering, and with a dispersion of 6.25 ps/ch. The overall shape of the pulse is Gaussian with a small "afterpulse" at about 250 ps. The plots illustrate the data-processing sequence: points for raw time-bin data; small dashes after subtraction of optical reflections from the surface of the flask; and the solid line for the final result after the IRF is deconvolved from the data. Both corrections reduce the amplitude of the afterpulse, and the deconvolution reduces the FWHM of the pulse from 175 to 155 ps. The reflection correction subtracts sequentially from each data point an amount that

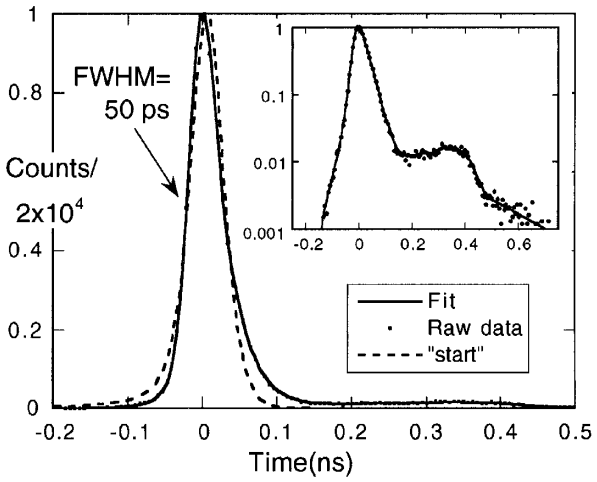

FIG. 2. Measurements of a 400-fs laser pulse (dots) define the overall IRF (solid line). The dashed curve shows "start" trigger jitter. The inset is a semilog plot of the IRF and data.

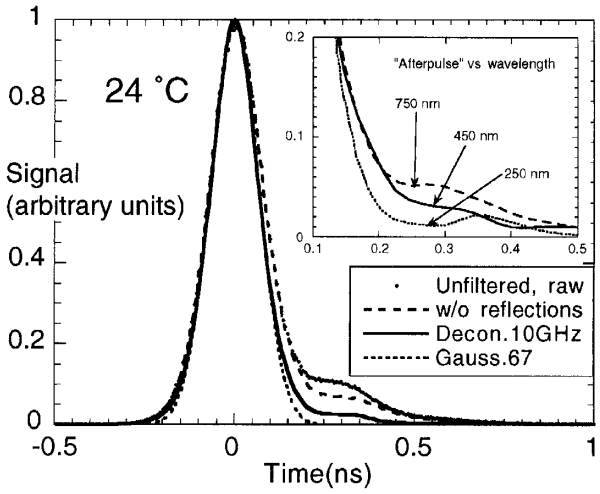

FIG. 3. SBSL FWHM is 155 ps at 24 °C, independent of wavelength. The inset shows deconvolved after pulses measured with three different optical filters.

is 3.5% (the reflection fraction) of the (corrected) data point 281 ps earlier (the flask optical transit time). For comparison purposes, the dotted line shows a Gaussian shape with a sigma of 67 ps (FWHM = 158 ps).

Careful deconvolution can extract a valid pulse shape from the data. Note that the deconvolution reduces the FWHM by about 20 ps, whereas subtracting the 50-ps IRF in quadrature (as often is done [4]) would reduce the width by less that 8 ps. The difference is that deconvolution corrects for the entire IRF, including the shoulder at about 350 ps (see Fig. 2). The deconvolution here uses a Fourier transform technique with a low-pass filter at 10 GHz. Higher-frequency cutoffs give similar results (with higher levels of noise), but lower cutoffs distort and broaden the pulse.

When the measurement is repeated with bandpass filters at 250, 400, 550, and 750 nm, the shape of the main pulse and its FWHM are unchanged from that shown in Fig. 3. However, some wavelength dependence is evident in the afterpulse. The inset in Fig. 3 shows the deconvolved shapes of afterpulses recorded with 250-, 450-, and 750-nm bandpass filters. The afterpulses are too broad and too strong to be reflections from the flask surface; they appear to be valid contributions to the actual SBSL pulse. The amplitude of the afterpulse is small, but the statistical accuracy of the data still is very good. The data show a trend toward earlier, stronger, and longer afterpulses for longer wavelengths. A portion of this trend may be due to spectral variations of the IRF, but available data suggest that this is not the case [5]. For times later than 400 ps, the intensity decays roughly exponentially, with a lifetime of about 155 ps.

Figure 4 shows the corrected and deconvolved SBSL pulse shapes recorded at 3 °C with the same bandpass filters. The rising halves of the pulses again are nearly Gaussian, but the shapes of the trailing edges vary with wavelength. The inset in Fig. 4, a semilog plot, shows that the decay of the pulse tail is nearly exponential, with an effective lifetime of about 125 ps.

The 3 °C pulse shapes in Fig. 4 show clear differences from the 24 °C data in Fig. 3. The 3 °C FWHM are greater, they increase for optical bands at longer wavelengths, and they decay slightly more rapidly. The general behavior of greater FWHM for longer wavelengths is highly reproducible, although some specific differences are small and not always reproducible. This is evident in the 400- and 550-nm data in Fig. 4, where the 400-nm FWHM is identical to that for 550 nm. The increase of pulse width with wavelength is most obvious for the 750-nm data. Over the course of numerous runs, the general trend of longer durations with longer wavelengths is consistent, with the 750-nm pulse width always significantly greater than for the other wavelengths.

The SBSL intensity at 3 °C is sufficient to produce good start pulses and generate reliable data over a 15% pressure range. Figure 5 shows the raw FWHM for pulse shapes measured through 250- and 750-nm filters, where the uncalibrated probe indicates relative pressure as mV of signal. The data show that the width increases by about 60 ps for a 15% increase in pressure, for both optical bands. These results are similar to those reported by Gompf for room-temperature measurements of FWHM vs acoustic pressure [3].

The data above show SBSL pulse durations that vary from about 150 to 300 ps, depending on experimental conditions. We have confirmed SBSL pulse lengths in this range with single-pulse measurements using a fast MCP and transient digitizer [7]. This pulse-width range is consistent with the results of Gompf [3] and Hiller [4]. Furthermore, recent streak-camera measurements of SBSL duration also find that SBSL duration is of the order of 200 ps [8]. The recent streak data also confirm our observation of slightly prolonged pulse tails. These pulse widths are consistent with previous reports of 50-ps

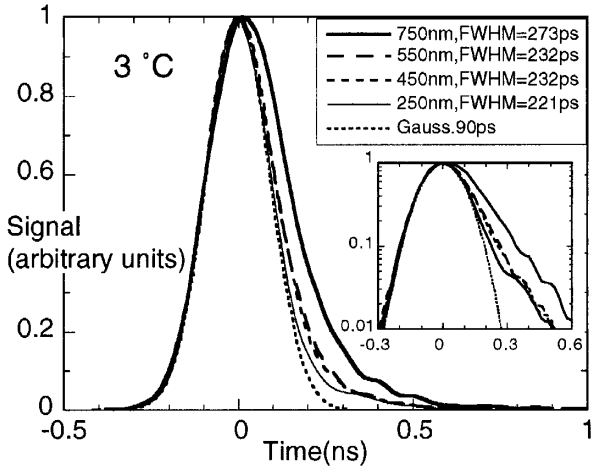

FIG. 4. SBSL FWHM at 3 °C increases with wavelength—especially in the far red at 750 nm. The inset is a semilog plot of the same data.

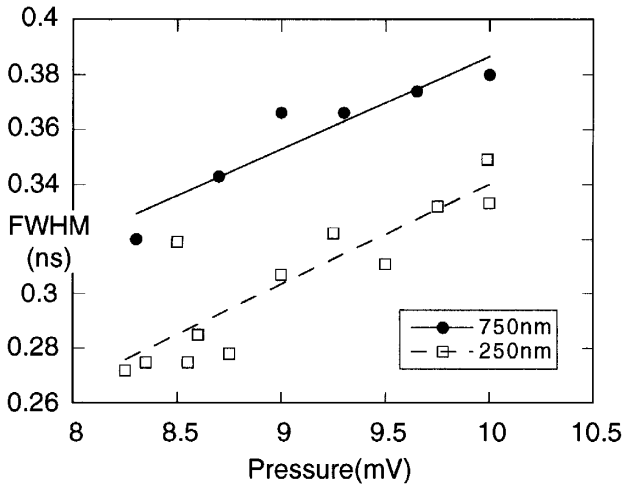

FIG. 5. SBSL FWHM increases by about 60 ps at both 250 and 750 nm for a 15% increase in acoustic pressure.

widths [9], and longer than our own report of a 15-ps width [10]. Our previous measurement was inferred from a 2-pixel-wide streak-camera image, which was recorded with good repeatability. We also reported that optical dispersion should have limited the streak system resolution to 30 ps. The only significant difference in apparatus was our previous use of a 20% glycerin/water mixture. Although the present results do not preclude shorter SBSL pulse widths, they suggest that the previous report of 15-ps pulse width was not correct, and that typical SBSL pulse widths tend to be significantly longer.

Together, these results establish a consistent description of SBSL pulse widths from tens to hundreds of ps. Given that TCPC is a sampling technique that measures average widths, independent confirmation from single-pulse measurements is important [7,8]. If SBSL pulse shapes are not repeated exactly on a pulse-to-pulse basis, then TCPC would measure an average pulse shape. This disadvantage is compensated by TCPC's high sensitivity that makes it possible to measure the dim SBSL flashes with excellent statistics and to follow minute changes in pulse shape.

Overall, these results demonstrate that the present TCPC method is a useful complement to other measurements of SBSL pulse shape. Improved statistics in the present data also make it possible to resolve characteristics such as a wavelength dependence of the 24 °C afterpulse and the exponential character of the emission decay. The wavelength dependence of the SBSL FWHM at 3 °C provides a distinct contrast with the room-temperature behavior.

These characteristics provide useful information as to the nature of SBSL emission mechanisms. Increased pulse width at longer wavelengths is consistent with simple thermal emission from a region that experiences a brief but extreme pulse of compression heating. Simply stated, this is because blackbody radiation extends to shorter wavelengths only as the source reaches higher temperatures. When such a source is heated and cooled by compression and expansion, emission of shorter wavelengths endures for shorter durations than for longer wavelengths.

Similarly, the spectral independence of the SBSL FWHM at 24 °C is difficult to explain in terms of thermal emission. If the emission is thermal, then it must be modified by other more subtle processes, such as time-dependent emissivities or opacities [11]. However, the wavelength independence might be indicative of some other emission mechanism. For example, broadband excimer emission by rare gases in the bubble would radiate simultaneously into a broad band of wavelengths, giving radiated pulse FWHM that would be independent of wavelength. Thus, the different spectral behaviors might indicate that more than one emission mechanism contributes to SBSL.

The small afterpulse at 300 ps demonstrates structure in the SBSL pulse shape beyond that of an asymmetric Gaussian. As spectral differences point to different emission mechanisms, temporal structure might be indicative of distinct hydrodynamic behavior in the collapsed bubble. For example, the model of Vuong and Szeri [12] predicts a brief heating of gas in the bubble associated with reflected waves or shocks after the main collapse. This prediction is roughly consistent with the afterpulse characteristics shown in Fig. 3: The emission is relatively weak, follows the main pulse, and it behaves like a thermal source in that longer wavelengths endure the longest.

In conclusion, TCPC reveals significant new spectral and temporal features of SBSL time dependence. The quality of data recorded by the present technique is limited by experimental stability and control. Further experiments that correlate SBSL pulse shape with parameters such as bubble radius acoustic drive pressure, and dissolved gas concentration could reveal spectral and temporal details of SBSL behavior. Holt and Gaitan have described an excellent example of multiparameter experiments of this type [13]. Such experiments have interfaced nicely with recent theoretical descriptions showing that bulk parameters such as dissolved gas concentrations, temperature, and acoustic drive are critically important to stable SBSL [14]. In this way, further experiments might be able to establish clear links to specific theoretical descriptions, and thus help to reach a fuller understanding of the nature and limitations of SBSL.

This work was performed under the auspices of the U.S. Department of Energy by the Lawrence Livermore National Laboratory under Contract No. W-7405-ENG-48.

[1] D. F. Gaitan *et al.,* J. Acoust. Soc. Am. **91**, 3166 (1992).
[2] For a comprehensive review of sonoluminescence and an extensive listing of pre-1997 references, see B. P. Barber *et al.,* Phys. Rep. **281**, 65 (1997).
[3] B. Gompf *et al.,* Phys. Rev. Lett. **79**, 1405 (1997).
[4] R. A. Hiller *et al.,* Phys. Rev. Lett. **80**, 1090 (1998).
[5] D. V. O'Connor and D. Phillips, *Time-correlated Single Photon Counting* (Academic, New York, 1984).
[6] For an extreme example of this problem, see R. A. Hiller and S. J. Putterman, Phys. Rev. Lett. **75**, 3549 (1995); **77**, 2345 (1996).
[7] M. Moran and D. Sweider (to be published).
[8] B. Gompf (personal communication); in Symposium on Sonoluminescence, Chicago, Illinois, 1997 (unpublished).
[9] B. P. Barber *et al.,* J. Acoust. Soc. Am. **91**, 3061 (1992).
[10] M. J. Moran *et al.,* Nucl. Instrum. Methods Phys. Res., Sect. B **96**, 651 (1995).
[11] W. C. Moss *et al.,* Science **276**, 1398 (1997).
[12] V. Q. Vuong and A. Szeri, Phys. Fluids **8**, 2354 (1996).
[13] R. G. Holt and D. F. Gaitan, Phys. Rev. Lett. **77**, 3791 (1996).
[14] S. Hilgenfeldt *et al.,* Phys. Fluids **8**, 2806 (1996); Phys. Rev. Lett. **80**, 1332 (1998).